J Geophys (1986) 60: 167–174

Journal of Geophysics

The retrieval of the seismic moment tensor from first-order perturbation theory and generation of compatible models

X. Lana[1] **and A.M. Correig**[1,2]

[1] Departament de Física de la Terra i del Cosmos, Facultad de Física, Universität de Barcelona, Diagonal 645, Barcelona 08028

[2] Laboratori d'Estudis Geofisics Eduard Fontserè, Institut d'Estudis Catalans, Carme, 47, Barcelona 08008

Abstract. The first-order perturbation theory applied to the eigenvectors and eigenvalues of the recovered seismic moment tensor give rise to a more accurate determination of the whole scalar seismic moment and allows a quantification of a possible superposition of distinct focal mechanisms, such as the double couple and the compensated linear vector dipole. On the other hand, the elements of the seismic moment tensor recovered from spectral amplitudes of shallow earthquakes will be obtained with important uncertainties, especially the M_{XZ} and M_{YZ} elements, when the starting models of inversion are close to pure normal, reverse or strike-slip faults. By using properties associated with the Lanczos matrix decomposition of the system of equations that defines the linearized inversion, a solution is given to the uncertainties of the seismic moment tensor elements. In such a way, a set of focal mechanisms, all fitting the experimental data, are generated and discussed in terms of other geophysical evidence. The applicability of the perturbation theory is tested by means of numerical simulation and applied to two earthquakes. For each earthquake, a set of models fitting the data has been generated. The vertical component of the Rayleigh wave spectral amplitudes, with periods ranging from 30 to 90 s, has been used.

Key words: Seismic moment tensor – Perturbation theory – Focal mechanism – Focal depth

Introduction

Following the pioneering work of Gilbert (1970), it is nowadays usual to retrieve the elements of the seismic moment tensor from seismic records. If spectral amplitudes and phases are available, the inversion process is linear and does not present special problems (Patton and Aki, 1979). However, except for a few well-studied regions of the Earth, phases can not be used because phase velocities must be known with an accuracy better than 0.5%, and the inversion has to be carried out with the amplitudes only. Mendiguren (1977) showed that using spectral amplitudes only, the inversion, which is no longer linear, is not unique. Moreover, the lack of uniqueness may be increased due to ill-conditioned systems (that appear when the initial trial solution is close to a reverse, normal or pure strike-slip fault) as well as errors in data (due to ambient noise, focusing, etc.) which may generate unrealistic spurious mechanisms.

In the present paper we study the problem of recovering the elements of the seismic moment tensor using only the amplitudes of the Rayleigh waves, vertical component, within a period range of 30–90 s. Periods shorter than 30 s have been avoided because of the difficulty of correction by attenuation as well as to avoid possible influences of directivity function (Correig and Mitchell, 1980), focusing and multipathing. Concretely, two problems are discussed: a quantification of the uncertainties of the seismic moment tensor and the influence of the lack of uniqueness on the focal mechanism obtained.

The uncertainties are quantified by applying first-order perturbation theory to the eigenvalues and eigenvectors of the seismic moment tensor. In order to carry out the process of inversion, the initial model is obtained by assuming a shear focal mechanism as deduced from the usual study of *P*-wave first motions. A first evaluation of the scalar seismic moment is made by dividing, at large periods, the recorded spectral amplitudes by the spectral amplitudes generated theoretically from the focal mechanism previously obtained with a unit scalar seismic moment.

We have found that perturbation theory is a useful instrument in recovering a correct scalar seismic moment. In addition, the existence of spurious focal mechanisms other than the double couple is also discussed through the study of the perturbed scalar seismic moment. The uncertainties associated with the focal mechanism are obtained from the perturbed eigenvectors and eigenvalues of the seismic moment tensor. The knowledge of the uncertainties of the focal mechanism is very important, for instance, when dealing with the orientation of the regional stress tensor (Angelier et al., 1982; Gephart and Forsyth, 1984). We show also that, in the case of moderate ambient noise, the correct focal depth corresponds to the depth for which the perturbation on the scalar seismic moment is a minimum.

The uniqueness is another parameter which we attempt to quantify. As a consequence of the lack of uniqueness, a badly constrained focal mechanism can be obtained. Using the properties of the matrix Lanczos decomposition applied to eigenvectors close to zero, a set of focal mechanisms that fit the observed data is analytically obtained as a function of the inversion residuals. This newly generated dataset is called "compatible models".

Offprint requests to: X. Lana

Perturbation theory

Following Knopoff and Randall (1970) we assume that the eigenvalues of the seismic moment tensor, obtained from an inversion process, can be interpreted as the superposition of a double couple (DC) and a compensated linear vector dipole (CLVD) in the following way:

$$\begin{pmatrix}\beta_1 & 0 & 0\\ 0 & \beta_2 & 0\\ 0 & 0 & \beta_3\end{pmatrix} = M_0(1-2f)\begin{pmatrix}1 & 0 & 0\\ 0 & -1 & 0\\ 0 & 0 & 0\end{pmatrix} +$$

$$M_0 2f\begin{pmatrix}1 & 0 & 0\\ 0 & -\frac{1}{2} & 0\\ 0 & 0 & -\frac{1}{2}\end{pmatrix} \qquad (1)$$

where β_i are the eigenvalues of the retrieved seismic moment tensor, M_0 the (scalar) seismic moment, $M_0(1-2f)$ gives the amount of seismic moment due to a DC mechanism [with eigenvalues (1, −1, 0)] and $M_0 2f$ gives the amount of seismic moment due to a CLVD mechanism [with eigenvalues (1, $\frac{1}{2}$, $-\frac{1}{2}$)]. f is a parameter defined as (Dziewonski and Woodhouse, 1983):

$$f = |\beta_3/\beta_1| \qquad (2)$$

with values ranging from 0 (pure DC) to $\frac{1}{2}$ (pure CLVD).

We apply first-order perturbation theory (Mathews and Walker, 1964) to eigenvectors and eigenvalues of the seismic moment tensor, in order to study the uncertainty associated with each mechanism. The method used to obtain the perturbed eigenvectors and eigenvalues is given in Appendix 1. The uncertainty in the mechanism is obtained as follows:

i) Let V_i' be the perturbed eigenvectors; following Mendiguren (1977) and Honda (1962), the perturbed principal axes of tension $\tilde{T}'$ and pressure $\tilde{P}'$ are given by:

$$\tilde{T}' = \pm V_1' \qquad \tilde{P}' = \pm V_2'. \qquad (3)$$

ii) Equations (1) and (2) define the perturbed (scalar) seismic moments as:

$$M_0' = \beta_1' \qquad M_{DC}' = \beta_1' + 2\beta_3' \qquad M_{CLVD}' = -2\beta_3'. \qquad (4)$$

Comparing the retrieved seismic moment with the computed perturbations, we can impose a criterion to decide which focal mechanism is representative and which is due to contaminating noise: the focal mechanism will be representative of a real physical process if the ratio M'/M is close to 1, where M is a (scalar) seismic moment (M_0, M_{DC} or M_{CLVD}) and M' is its perturbed value. The term "close to 1" will be quantified in the numerical simulations and applications.

iii) Following Strelitz (1980), it is also possible to compute the angle between the eigenvector V_i and the perturbed eigenvector V_j' as:

$$C_{ij} = \cos(V_i \cdot V_j'). \qquad (5)$$

This angle C_{ij} represents the confidence ellipse of pressure, tension and null vector axis, projected on the focal sphere.

Generation of compatible models of mechanisms

Let

$$\delta D = A\,\delta P + \varepsilon \qquad (6)$$

be the system of equations from which we have computed the elements of the seismic moment tensor, where A is the matrix of partial derivatives of the spectral amplitudes with respect to the parameters of inversion (defined in Appendix 2) δD the difference vector between observations and predictions from an initial model P_0, δP is the correction to P_0 and ε is the error vector associated with the observations. A solution of system (6), due to the existence of ε, will be one that minimizes:

$$E = \|D - AP'\| \qquad (7)$$

where D are the observed spectral amplitudes and E the Euclidian norm of residuals of inversion. P' is the solution that minimizes Eq. (7).

The solution P' which minimizes Eq. (7) is not unique, because by solving Eq. (6) according to the decomposition of Lanczos (1961) of A in eigenvalues μ_i and eigenvectors (U_i, V_i), another possible solution is:

$$P^* = P' + P \qquad (8)$$

where:

$$P = \sum_i \alpha_i U_i \qquad (9)$$

is a linear combination of the eigenvectors U_i of A, associated with eigenvalues close to zero. Note that the complete set of eigenvectors U_i generates the parameter space. Taking this into account, our problem may now be formulated in a different way: finding a set of solutions P which satisfy:

$$\|AP' - AP^*\| \leqq Q \qquad (10)$$

where Q is a value to be determined as a function of the Euclidian norm E. Expression (10) can be interpreted in the following way: because the eigenvectors U_i are associated with eigenvalues close to zero, the set of models P that satisfy (10) will predict the observed amplitudes D with the same accuracy as model P', solution of Eq. (7). This assessment is a consequence of the existence of the term ε in Eq. (6) and the residuals of the inversion.

To obtain maximized values of P^*, the coefficients α_i of Eq. (9) have to be computed. Using (8) and (9), expression (10) can be rewritten as:

$$\sum_i (\mu_i \alpha_i)^2 \leqq Q. \qquad (11)$$

From a geometrical point of view, expression (11) represents a hyperellipsoid with semiaxes $\mu_i Q^{\frac{1}{2}}$. The computation of the coefficients which maximize P is equivalent to searching the tangency point between the hyperellipsoid (11) and the hyperplane (9). Application of this concept gives rise to the expression:

$$(\alpha_i)_{\max} = \pm \frac{Q^{\frac{1}{2}}}{\left\{\sum_j \left\{\frac{V_{jk}\,\mu_i^2}{V_{ik}\,\mu_j}\right\}^2\right\}^{\frac{1}{2}}} \qquad (12)$$

where n is the number of parameters and $(\alpha_i)_{\max.}$ is the coefficient that, substituted in (9), maximizes the component k of vector P that satisfies (10), and V_{jk} the component k of the eigenvector V_j. For a discussion on the parameter Q see the applications given below and a recent paper of

Table 1. Numerical simulation. Case S is an example of noise-free signal. Cases S 1, S 2 and S 3 are signals contaminated with background noise. S 4 is an example of signal contaminated by multiplicative noise. M_{DC}/M_0 gives the ratio of shear focal mechanism with respect to the whole focal mechanism. The percentage of perturbation in M_0, M_{DC} and M_{CLVD} is given by $\%M_0$, $\%M_{DC}$ and $\%M_{CLVD}$, respectively. The scalar seismic moment tensor is given in units of 1.0 E+16 Nm. Focal depth is given in kilometers. The signal-to-noise ratio is also given

Focal depth	M_0	M_{DC}	M_{CLVD}	M_{DC}/M_0	$\%M_0$	$\%M_{DC}$	$\%M_{CLVD}$
Case S							
7.5	95.4	47.8	47.6	0.50	8.8	39.8	23.0
10.5	132.0	57.8	74.2	0.44	12.8	69.2	18.9
13.5	100.0	99.8	0.2	0.99	0.5	0.9	94.5
16.5	124.0	103.0	21.0	0.83	8.2	4.5	26.6
Case S 1							
7.5	95.7	48.2	47.5	0.50	9.0	39.4	23.0
10.5	132.7	57.8	74.9	0.44	12.2	51.5	18.2
13.5	101.0	99.4	1.6	0.99	0.9	1.7	87.5
16.5	213.0	108.0	105.0	0.51	17.3	34.0	22.8
Case S 2							
7.5	96.3	49.1	47.9	0.51	9.6	41.1	25.0
10.5	134.2	58.0	76.2	0.43	11.5	50.0	18.4
13.5	102.7	98.0	4.7	0.95	3.0	5.5	95.0
16.5	216.0	109.0	107.0	0.50	16.8	55.9	22.0
Case S 3							
7.5	100.0	54.2	45.8	0.54	7.1	34.0	22.3
10.5	143.0	60.6	82.4	0.43	7.8	44.1	16.3
13.5	164.0	34.8	129.2	0.21	14.6	70.3	14.0
16.5	232.0	113.0	119.0	0.48	14.1	57.4	27.3
Case S 4							
7.5	96.0	48.2	47.2	0.50	11.8	37.3	33.8
10.5	132.0	61.0	71.0	0.46	17.5	65.3	22.5
13.5	104.0	50.1	53.9	0.48	58.7	72.3	25.4
16.5	213.0	105.0	108.0	0.49	55.4	69.3	25.2

	Signal/noise ratio					
Period	60 s	50 s	40 s	35 s	30 s	25 s
Case S1	10	20	25	50	75	75
Case S2	2	4	5	10	25	25
Case S3	1	1	1	2	5	5

Pous et al. (1985). It is important to point out that, from Eq. (9), we will obtain as many maximized solutions P as parameters that define the model, five in our case. Moreover, in the computation of P, Eq. (12) gives stronger weight to the smaller eigenvalues; for this reason the addition that appears in (9) can be extended to the total number of parameters.

Numerical simulation

In order to study the uncertainty in the M_0, M_{DC}, M_{CLVD} scalar seismic moments, and focal depth determination due to ambient noise, some numerical simulations have been carried out. Synthetic spectral seismograms, with periods ranging from 25 to 60 s, have been generated (case S) for a pure double couple shear fault, located at a depth of 13.5 km with the following parameters: dip = 45°, slip = 45°, strike = 80° (clockwise from north) and a scalar seismic moment of 1.0 E+18 Nm. As a propagating medium, we use the model of Dziewonski and Anderson (1981). The ambient noise of the seismograms pretend to be randomly distributed values ranging from −1 to +1, added to the real and to the imaginary parts of the spectra and multiplied by three increasing levels of signal-to-noise ratio. These levels of signal-to-noise ratio are similar to those used in Patton and Aki (1979), which were obtained by studying the spectral components of several sets of background noise recorded at WWSSN stations. Corresponding results have been named cases S 1, S 2 and S 3. The signal-to-noise ratios for periods within 25–60 s are given in Table 1. Besides this, possible existing lateral inhomogeneities have been simulated by random multiplications or divisions of the spectral amplitudes by a factor of 0.7; (case S 4). The focusing and multipathing effects can be generated by random multiplications or divisions of spectral amplitudes by a factor dependent on frequency for periods lower than 30 s. This possibility will not be taken into consideration because the process of inversion has been applied to periods greater than 30 s. In doing so, we have avoided the influence of multipathing focusing, attenuation and finite extension of the seismic source. As a counterweight to this situation, there will exist some loss of resolution in the focal depth determination, especially when there is very important seismic noise. In Fig. 1, logarithms of some spectral amplitudes in dyne cm reduced to the source with an arbitrary azimuth are shown, corresponding to cases S 1, S 3 and S 4.

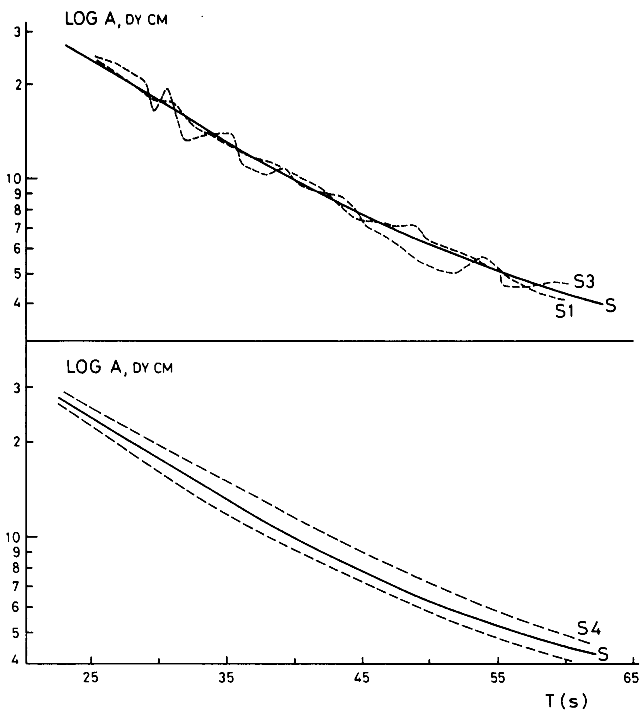

Fig. 1. Synthetic spectral amplitudes of the vertical component reduced to the seismic source for an arbitrary azimuth. Case S corresponds to signal without noise. Case S 1 corresponds to signal contaminated with the first level of noise in Table 1. Case S 3 corresponds to signal contaminated with the third level of noise in Table 1. *Dashed lines* (cases S4) correspond to maximum variations in the spectral amplitude when multiplicative noise is present

The process of retrieving focal mechanisms for a noise-free spectrum (case S) and contaminated spectra (cases S1, S2, S3 and S4) was carried out in a previous work (Lana and Correig, 1985), minimizing the residual of the inversion and the standard deviation of the first parameter of inversion (defined in Appendix 2). For cases S, S1 and S2 the correct focal depth of 13.5 km was obtained, whereas the retrieved focal depth for cases S3 and S4, obtained from the minimum standard deviation of P_1, was 7.5 km.

In the present study the numerical simulation has been carried out by applying only the perturbation theory. The algorithm of mechanism generation in perturbation theory will be applied, later on, to two real events. The inversion process is repeated for several depths and perturbation theory is applied to each one. In Table 1 the retrieved seismic moments (M_0, M_{DC} and M_{CLVD}) are summarized, as well as the percentage of perturbation for every seismic moment ($\%M_0$, $\%M_{DC}$, $\%M_{CLVD}$) and the ratio M_{DC}/M_0 for the five cases S to S4. It is stated for cases S, S1 and S2 that not only the residuals and standard deviations are minimal, but the ratio M_{DC}/M_0 is a maximum for this focal depth, the percentage associated with perturbation of M_0 and M_{DC} is a minimum and the component M_{CLVD} of the mechanism makes no sense because the associated perturbation is too large. For cases S3 and S4, the ratio M_{DC}/M_0 is a maximum for a focal depth of 7.5 km and the perturbation percentage of M_0 and M_{DC} are minimum. We can conclude that for a poor signal-to-noise ratio, such as in case S3, and for relatively high multiplicative noise, case S4, the scalar seismic moment M_0 is retrieved with enough accuracy and a spurious focal depth, with an error of approximately 6 km, is recovered. We also obtain the CLVD component of the focal mechanism with moderate uncertainties. In short, in cases S3 and S4 there are some uncertainties concerning the correct focal depths and focal mechanism components, but the whole scalar seismic moment M_0, which gives information about the strength of the seismic event, is well recovered.

Applications

Perturbation theory and the computation of compatible mechanisms has been applied to two earthquakes: event January 1, 1965 (MED) and event November 18, 1970 (PAC). Focal mechanisms for both earthquakes were previously studied by Lana and Correig (1985) by means of the retrieval of the elements of the seismic moment tensor. Table 2a shows information obtained from NEIS agency; azimuthal distribution and epicentral distances of the WWSSN stations used. Due to the moderate magnitude of both earthquakes, the seismic signal is poorly recorded at some WWSSN stations and the azimuthal distribution is not entirely fulfilled. Figure 2 shows several vertical-component seismograms for event PAC. Table 2b shows the focal parameters, elements of the seismic moment tensor, focal mechanism and focal depth for both earthquakes as reported by Lana and Correig (1985).

In the study of residuals, focal depth showed some uncertainty which could be resolved for event MED by searching for a minimum of the standard deviations of parameter P_1 associated with the real part of the spectra. The study of the P_1 standard deviations for several depths is entirely coherent because P_1 is the only parameter depending explicitly on the focal depth according to the functions G_1 and G_2. However, an uncertainty in the focal depth was obtained (Lana and Correig, 1985) for event PAC, studying the residuals and the standard deviation of parameter P_1. This situation could be associated with the ill-conditioned system result of an initial model for event PAC close to a pure strike-slip fault. The poor dependence on the focal depth of the standard deviation of P_1 remains unexplained because a better resolution of the focal depth is expected by studying the parameters associated with the real part of the spectral amplitudes.

Table 2a. Information available from NEIS agency (approximate focal depth, location, origin time and magnitude) WWSSN stations, epicentral distances in km, and azimuth clockwise from north

Event:	MED (35.7°N, 4.4°E)	PAC (28.7°S, 112.7°W)
Date:	January 1, 1965	November 18, 1970
Focal depth:	10 km	5 km
Magnitude:	5.2 (*mb*)	5.6 (*mb*)
WWSSN stations	Epicentral distance	azimuth
Event MED		
PTO	1,284.3	301.9
AKU	3,560.6	343.0
COP	2,305.2	12.9
ESK	2,257.8	347.4
KEV	4,033.9	13.1
STU	1,506.9	13.9
TOL	876.5	304.5
VAL	2,146.7	331.7
AQU	1,073.6	43.8
ATH	1,738.4	75.9
PDA	2,476.1	285.6
Event PAC		
BKS	7,430.6	352.1
LON	8,400.1	353.5
QUI	3,983.3	69.9
NNA	4,148.5	71.0
TUC	6,742.0	1.8
COR	8,180.5	352.1
LPS	5,384.4	31.2
ARE	4,421.4	81.2
PEL	4,018.7	107.8
LEM	14,176.8	234.1
MAT	13,451.3	297.4

Table 2b. Elements of the seismic moment tensor, focal depth, dip, slip, strike and scalar seismic moment (M_{DC}) for the double couple focal mechanism (Lana and Correig, 1985)

Event PAC		
$M_{XX}=-0.86$ E+18	$M_{XY}=0.21$ E+18	$M_{XZ}=-0.10$ E+14
$M_{YY}=1.10$ E+18	$M_{YZ}=0.10$ E+14	$M_{ZZ}=-0.24$ E+18
Dip = 90°	Slip = 0°	Strike = N 51° E
$M_{DC}=0.65$ E+18 Nm		Depth: 0–30 km
Event MED		
$M_{XX}=-0.38$ E+18	$M_{XY}=0.13$ E+18	$M_{XZ}=-0.11$ E+17
$M_{YY}=0.95$ E+17	$M_{YZ}=0.51$ E+18	$M_{ZZ}=0.29$ E+18
Dip = 48.9°	Slip = 70.1°	Strike = N 29° E
$M_{DC}=0.54$ E+18 Nm		Depth: 10.5 km

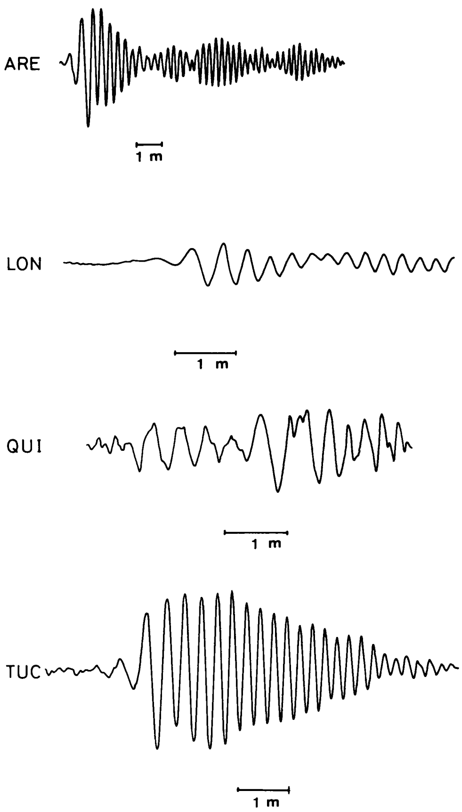

Fig. 2. Long-period vertical-component records of event PAC at WWSSN stations LON, TUC, QUI, ARE

In Table 3 there is a summary of results obtained from perturbation theory; a focal depth of 10.5 km for event MED is confirmed. For event PAC, the uncertainty is less than in the previous results, and we conclude a focal depth of 4.5 km. Although the percentage of shear mechanism for event PAC is practically the same for a focal depth of 4.5 km as for 7.5 km, the perturbation in the M_{DC} seismic moment is smaller at a focal depth of 4.5 km. The focal depth obtained for the two events ware very similar to those reported by NEIS agency. It is important to note that in both events the possible CLVD mechanism for the assumed focal depth is obtained with a very large perturbation in their seismic moment; for this reason we conclude that it is not representative of the physical process at the seismic source.

Angles C_{ij} formed by perturbed and unperturbed eigenvectors of the mechanism are listed in Table 4 for both events. It can be seen that the uncertainty in the orientation of the null, compressional and tensional axes ranges between 0° and 5°. We can conclude that the uncertainty in the orientation of the principal axes is small and, consequently, the strike, dip and slip of the DC mechanisms will be accurately obtained.

The algorithm of generation of compatible models has been applied to events MED and PAC when the elements of the seismic moment tensor, the scalar seismic moment and the focal depth have been well delimited. The criterion we have considered, for deciding whether a model is compatible with that obtained by generalized inversion or not, imposes that the square error between the amplitudes used in the inversion and those given by compatible models generated by Eq. (11) should be, in the worst case, as large

Table 3. Results obtained by applying perturbation theory. M_{DC}/M_0 gives the ratio of shear mechanism with respect to the whole mechanism. The percentage of perturbation in the scalar seismic moments is given by $\%M_0$, $\%M_{DC}$ and $\%M_{CLVD}$. The scalar seismic moment is given in units of 1.0 E+16 Nm. The focal depth is given in kilometers

Focal depth	M_0	$\%M_0$	M_{DC}	$\%M_{DC}$	M_{CLVD}	$\%M_{CLVD}$	M_{DC}/M_0
Event PAC							
4.5	1.12	8.2	0.65	5.9	0.47	20.1	0.58
7.5	1.23	12.2	0.67	8.3	0.56	23.2	0.54
10.5	1.35	15.3	0.70	13.5	0.65	28.4	0.52
13.5	1.49	27.2	0.72	18.4	0.77	32.3	0.48
16.5	1.64	32.5	0.81	22.6	0.83	37.9	0.49
19.5	1.85	35.1	0.84	28.0	1.01	42.1	0.45
Event MED							
7.5	0.34	26.5	0.08	3.8	0.26	38.5	0.23
10.5	0.62	10.1	0.54	17.0	0.08	72.3	0.88
13.5	0.42	13.3	0.19	22.1	0.23	44.8	0.46
16.5	0.47	46.0	0.31	25.5	0.16	46.6	0.66
19.5	0.41	53.4	0.35	30.2	0.06	85.3	0.85

Table 4. Angles between perturbed and unperturbed principal axes of the two earthquakes. In the absence of perturbation, the angles will be equal to 90°. C_{ij} is the angle between the unperturbed vector *i* and the perturbed vector *j*, with *i* different to *j*

	Event PAC	Event MED
C_{12}	89.95°	95.17°
C_{21}	90.50°	90.18°
C_{13}	89.96°	85.03°
C_{31}	89.95°	93.97°
C_{23}	89.32°	88.92°
C_{32}	89.95°	88.40°

as the residual E of the inversion. The first approximate value of Q may be assumed to be the residual E of the inversion. We will have to reduce the assumed value of Q until the condition of linearity, implicit in the derivation of (11), is satisfied, because our system is not linear, although it has been linearized in (6).

Since P is obtained as a linear combination of eigenvectors associated with very small eigenvalues of the Lanczos (1961) decomposition, it is reasonable to expect important deviations in models generated from event PAC for which two eigenvalues close to zero have been obtained in all steps of the inversion process. For event MED none of the obtained eigenvectors is too small, so the obtained compatible models will not really differ from that obtained by inversion.

A similar situation to that obtained for event PAC has been reported by Kanamori and Given (1981) in an inversion study of the real and imaginary parts of the spectra corresponding to very superficial earthquakes. To avoid an ill-conditioned system, those authors impose the condition that parameters P_4 and P_5 (see Appendix 2) are zero. Once the inversion is performed, they try to determine the values of parameters P_4 and P_5 from geological or geophysical information. From the point of view of the present study, we solve this problem by first generating the maximized

Table 5. Increments of P parameters (see Appendix 2) that maximize the five compatible models for events PAC and MED

Components	(1)	(2)	(3)	(4)	(5)
Event PAC					
Model 1	0.160 E+08	−0.942 E+09	−0.123 E+09	−0.393 E+12	−0.685 E+18
Model 2	−0.101 E+08	0.149 E+10	−0.154 E+09	−0.729 E+12	0.631 E+18
Model 3	−0.246 E+07	−0.287 E+09	0.799 E+09	−0.142 E+12	0.130 E+16
Model 4	−0.907 E+04	−0.157 E+09	−0.164 E+06	0.693 E+15	−0.124 E+15
Model 5	−0.139 E+08	0.119 E+09	0.132 E+07	−0.109 E+12	0.787 E+18
Event MED					
Model 1	0.418 E+14	0.192 E+16	0.659 E+15	0.300 E+15	−0.414 E+15
Model 2	0.224 E+14	0.357 E+16	0.419 E+15	0.997 E+14	−0.346 E+15
Model 3	0.133 E+14	0.720 E+15	0.206 E+15	−0.669 E+15	0.185 E+16
Model 4	0.352 E+13	0.998 E+15	−0.387 E+15	0.357 E+16	−0.149 E+16
Model 5	−0.294 E+13	−0.210 E+15	0.649 E+15	−0.904 E+15	0.589 E+16

Table 6. Shear focal mechanism and whole scalar seismic moment for the five maximized compatible models obtained for event PAC. Models 1, 2 and 5 correspond to a normal fault. Models 3 and 4 correspond to a pure strike-slip fault. Strike is given clockwise from north

	M_0(Nm)	M_{DC}(Nm)	Dip	Slip	Strike
Event PAC					
Model 1	1.31 E+18	0.94 E+18	64.9°	−21.6°	56.1°
Model 2	1.26 E+18	0.98 E+18	65.9°	−21.9°	57.8°
Model 3	1.12 E+18	0.65 E+18	89.9°	0.0°	51.0°
Model 4	1.12 E+18	0.64 E+18	89.9°	0.0°	51.4°
Model 5	1.40 E+18	0.85 E+18	63.4°	−22.2°	56.8°

models compatible with observations and, in a second step, we select the model that fits other geophysical and geological data best. Note that there is no need to make parameters P_4 and P_5 zero, although in the case of an ill-conditioned system no variation of those parameters are allowed.

In Table 5 there is a list of the five series of increments in P that generate the maximized compatible models for both events. We can clearly see that only for event PAC are compatible models, well differentiated from that of inversion, obtained; especially for parameters P_4 and P_5, the values of which zero at the initial model P_0. Table 6 shows the maximized generated compatible models for event PAC. We can clearly see that two solutions are possible. Models 3 and 4 represent a strike-slip fault, whereas models 1, 2 and 5 represent a normal fault. On the other hand, the strike angle is practically the same for all the models. The strike-slip solution agrees with that obtained by Forsyth (1972), who locates this event on a transform fault. If this is the case, the strike-slip solution is the correct one. However, the percentage of DC mechanism with respect to total mechanism is higher for the normal fault solution. Because there is no evidence of a CLVD mechanism, the normal fault solution could be favoured.

The maximized compatible models for event MED are not included in Table 6 because the increments of P in Table 5 are very small with respect to the parameters P obtained in the inversion. Consequently, the compatible strike, dip, slip and seismic moments are very close to those shown in Table 2a.

Conclusions

Perturbation theory has been applied to the retrieval of the scalar seismic moment of earthquakes. Through numerical examples and applications to two previously studied earthquakes, perturbation theory appears to be a powerful method in improving the scalar seismic moment M_0 and in discussing the physical meaning of focal mechanisms different to the DC model. The focal depth determination is also improved in some cases. When different kinds of noise contaminate the seismic signals, the applicability of the perturbation theory to the recovery of very exact focal depths is restricted.

The generation of compatible models is especially useful in solutions where the lack of resolution affects some inversion parameters. These solutions will appear when the initial models are close to pure normal, reverse and strike-slip faults, generating ill-conditioned systems. By applying this algorithm of generation, we are able to obtain a large set of models. These models fit the observations as well as models obtained by inversion, although they represent different focal solutions. Once this large set of possible models has been obtained, it is straightforward to incorporate data from other sources to delimit realistic seismic source models.

Appendix 1

Let M be the seismic moment tensor obtained by inversion of spectral amplitudes of Rayleigh waves, and let δM be the tensor whose elements are a function of the standard deviations $\sigma(M_{ij})$ associated with each element M_{ij}.

Let us define the perturbed seismic moment as:

$$M' = M + \delta M \tag{13}$$

where

$$\delta M_{ij} = \sigma(M_{ij}) g_{ij} \tag{14}$$

and g_{ij} is a gaussian variable with zero mean and unit standard deviation.

Following Mathews and Walker (1964), the perturbed eigenvalues β'_i and eigenvectors V'_i, assuming that the eigenvalues are not degenerated, are given by:

$$V'_j = V_j + \sum_k a_{kj} V_k, \tag{15}$$

$$\beta'_j = \beta_j + V_j \, \delta M \, V_j \tag{16}$$

where:

$$a_{kj} = V_k \, \delta M \, V_j / (\beta_k - \beta_j), \quad j \neq k \tag{17}$$

and V_j and β_j are the unperturbed eigenvectors and eigenvalues, respectively.

From a statistical point of view, we are interested in computing the expected value of $\|a_{kj}\|$ that can be expressed as:

$$E(\|a_{kj}\|) = \{ \sum_{s,t,l,m} V_{ks} V_{jt} V_{lj} V_{mn} E(\delta M_{lm} \delta M_{st}) / (\beta_k - \beta_j)^2 \}^c \tag{18}$$

where V_{ij} means the component j of vector V_i. $\delta M_{lm} \delta M_{st}$ may be interpreted as a fourth-order tensor which, if $st = lm$, give us the covariance of M_{lm} and, if $st \neq lm$, give us the correlation between M_{lm} and M_{st}.

Assuming that the correlation between M_{lm} and M_{st} is small, implying that $E(\delta M_{lm} \delta M_{st})$ are close to zero, we get:

$$E(\|a_{kj}\|) = \{ \sum_{l,t} (V_{lk} V_{tj} \delta M_{lt})^2 / (\beta_k - \beta_j)^2 \}^{\frac{1}{2}} \tag{19}$$

and the expected value of the perturbed eigenvalue is given by:

$$E(\beta'_j) = \beta_j + \{ \sum_{l,t} (V_{lj} V_{tj} \delta M_{lt})^2 \}^{\frac{1}{2}}. \tag{20}$$

Similarly, the expected value of the perturbed eigenvector can be expressed as:

$$E(V'_j) = V_j + \sum_k V_k E(\|a_{kj}\|), \quad k \neq j. \tag{21}$$

Appendix 2

Let

$$U_n = M_{pq}(w) \, {}_{Gnp,q}(w) \tag{22}$$

be the spectral displacement field, expressed as a product of the seismic moment tensor by the derivative of the Green's function of the medium with respect to spatial coordinates (Aki and Richards, 1980).

Following Mendiguren and Aki (1978), if we develop Eq. (22) with as many equations as different azimuths for which we have observations, we can resolve the following five parameters:

$$\begin{aligned} P_1 &= (M_{xx} + M_{yy}) G_1 + M_{zz} G_2 \\ P_2 &= M_{yy} - M_{xx} \\ P_3 &= M_{xy} \\ P_4 &= M_{yz} \\ P_5 &= M_{xz} \end{aligned} \tag{23}$$

where G_1 and G_2 are functions that depend of the medium structure, stress and displacement functions and focal depth (Takeuchi and Saito, 1972).

The covariance matrix of the parameters of inversion is:

$$\mathrm{Cov}(P) = A^{-1} \phi (A^{-1})^T \tag{24}$$

where A^{-1} is the generalized inverse of matrix A of Eq. (6) (Lanczos, 1961) and ϕ is the covariance matrix of associated errors of Eq. (6). From Eq. (23) it can be seen that only the covariances of M_{xy}, M_{yz} and M_{xz} can be computed. The following process can be devised to compute the remaining terms. By imposing that the trace of the tensor be zero, and using the definitions of P_1 and P_2 [Eq. (23)], the following system can be written down:

$$\begin{pmatrix} P_1 \\ P_2 \\ 0 \end{pmatrix} = \begin{pmatrix} G_1 & G_1 & G_2 \\ -1 & 1 & 0 \\ 1 & 1 & 1 \end{pmatrix} + \begin{pmatrix} M_{xx} \\ M_{yy} \\ M_{zz} \end{pmatrix} + \varepsilon \tag{25}$$

where ε are the uncertainties associated with P_1 and P_2. By writing the covariance matrix of ε as:

$$\mathrm{Cov}(\varepsilon) = \begin{pmatrix} C_{11} & C_{12} & 0 \\ C_{21} & C_{22} & 0 \\ 0 & 0 & 0 \end{pmatrix} \tag{26}$$

where C_{ij} is the covariance matrix of P_1 and P_2, and using (24), one gets the following expression for the covariance of M_{xx}, M_{yy}, M_{zz}:

$$\begin{aligned} &\mathrm{Cov}(M_{xx}, M_{xx}) = (C_{11} - 2C_{12} G + C_{22} G^2) G' \\ &\mathrm{Cov}(M_{yy}, M_{yy}) = (C_{11} + 2C_{12} G + C_{22} G^2) G' \\ &\mathrm{Cov}(M_{zz}, M_{zz}) = 4C_{11} G' \\ &\mathrm{Cov}(M_{xx}, M_{yy}) = \mathrm{Cov}(M_{yy}, M_{xx}) = (C_{11} - C_{22} G^2) G' \\ &\mathrm{Cov}(M_{zz}, M_{xx}) = \mathrm{Cov}(M_{xx}, M_{zz}) = (-2C_{11} + 2C_{12} G^2) G' \\ &\mathrm{Cov}(M_{yy}, M_{zz}) = \mathrm{Cov}(M_{zz}, M_{yy}) = (-2C_{11} - 2C_{12} G^2) G' \end{aligned} \tag{27}$$

where $G = (G_1 - G_2)$ and $G' = G^{-2}/4$.

Acknowledgements. Enric Banda read the manuscript and made valuable suggestions.

References

Aki, K., Richards, P.G.: Quantitative sesimology. Theory and methods, vol. I. San Francisco: Freeman, E.W. 1980

Angelier, J., Tarantola, A., Valette, B., Manoussis, S.: Inversion of field data in fault tectonics to obtain the regional stress. I. Single phase populations: a new method of computing the stress tensor. Geophys. J.R. Astron. Soc. **69**, 607–621, 1982

Correig, A.M., Mitchell, B.: Regional variation of Rayleigh wave attenuation coefficients in the Eastern Pacific. Pure Appl. Geophys. **118**(3), 831–845, 1980

Dziewonski, A.M., Anderson, D.L.: Preliminary reference Earth model. Phys. Earth Planet. Inter. **25**, 297–356, 1981

Dziewonski, A.M., Woodhouse, H.: An experiment in systematic global seismicity: centroid moment tensor solutions for 201 moderate and large earthquakes of 1981. J. Geophys. Res. **88**, 3247–3272, 1983

Forsyth, D.W.: Mechanisms of earthquakes and plate motions in the East Pacific. Earth Planet. Sci. Lett. **17**, 189–193, 1972

Gephart, J.W., Forsyth, D.W.: An improved method for determining the regional stress tensors using earthquake focal mechanism data: application to the San Fernando earthquake sequence. J. Geophys. Res. **89**, 9305–9320, 1984

Gilbert, F.: Excitation of normal modes of the Earth by earthquakes sources. Geophys. J. R. Astron. Soc. **22**, 223–226, 1970

Honda, H.: Earthquake mechanism and seismic waves. J. Phys. Earth **10**(2), 1–98, 1962

Kanamori, H., Given, J.W.: Use of long period surface waves for rapid determination of earthquake source parameters. Phys. Earth Planet. Inter. **27**, 8–31, 1981

Knopoff, L., Randall, M.J.: The compensated linear vector dipole: a possible mechanism for deep earthquakes. J. Geophys. Res. **75**, 4957–4963, 1970

Lana, X., Correig, A.M.: Determinación de mecanismos focales y profundidades focales mediante la inversion linealizada del tensor de momento sísmico. Rev. de Geofisica **41**(1), 37–51, 1985

Lanczos, C.: Linear differential operators. London: Van Nostrand Co. 1961

Mathews, J., Walker, R.: Mathematical methods of physics. Menlo Park (California): Benjamin 1964

Mendiguren, J.A.: Inversion of surface wave data in source mechanism studies. J. Geophys. Res. **82**, 889–894, 1977

Mendiguren, J.A., Aki, K.: Source mechanism of deep Colombian earthquake of July 31, 1970 from free oscillation data. Geophys. J. R. Astron. Soc. **55**, 539–556, 1978

Patton, H., Aki, K.: Bias in the estimate of the seismic moment tensor by the linear inversion method. Geophys. J. R. Astron. Soc. **59**, 479–495, 1979

Pous, J., Lana, X., Correig, A.M.: Generation of Earth stratified models compatible with both ellipticity and phase velocity observations of Rayleigh waves. Pure Appl. Geophys. **123**, 1985 (in press)

Strelitz, R.A.: The fate of the downgoing slab: a study of the moment tensor from body waves of complex deep focus earthquakes. Phys. Earth Planet. Inter. **21**, 83–96, 1980

Takeuchi, H., Saito, M.: Seismic surface waves. Methods in computational physics (11), 217–303, Academic Press 1972

Received April 2, 1985; revised version July 20, 1986
Accepted October 19, 1986